DOI: 10.1002/ange.200503011

Uniformly *a*-Oriented MFI Zeolite Films by Secondary Growth**

*Jungkyu Choi, Shubhajit Ghosh, Zhiping Lai, and Michael Tsapatsis**

Molecular-sieve thin films are attracting research interest because of emerging applications as membranes,[1–6] chemical sensors,[7–9] low-*k* dielectrics,[10] and hosts for supramolecular organization of guest molecules and/or stabilization of guest nanostructures.[11–14] Siliceous ZSM-5 ($Si_{98}O_{196}$-ZSM-5; structure type MFI) films, from now on referred to as MFI films, are studied widely because they serve as a model system and hold promise for practical applications.[15–19] For example, MFI membranes are ideally suited for separating xylene isomers, since the pore size of the MFI framework should allow *p*-xylene (kinetic diameter ca. 5.8 Å) to permeate relatively fast, while the bulkier *o*- and *m*-xylene (kinetic diameters ca. 6.8 Å) should permeate at a much lower rate. The separation of xylene isomers is important in the petrochemical industry, since they are widely used as industrial solvents and precursors. Separations based on MFI membranes could be a better alternative to current technology that is based on energy-intensive operations such as fractional crystallization, adsorption in a simulated moving bed, and distillation. Among other microstructural characteristics, the preferred orientation correlates strongly with film performance, and therefore controlling the preferred orientation is important.[20,21] Although continuous MFI films with certain types of preferred orientation have been reported,[22–39] a method that allows systematic manipulation of molecular-sieve pore orientation in supported, thin, continuous films has not been demonstrated.

Syntheses of MFI membranes described recently can be broadly classified into two categories: in situ and secondary (or seeded) growth. In the in situ technique, the support surface is directly contacted with an alkaline solution containing the zeolite precursors and subjected to hydrothermal conditions. Under appropriate conditions, zeolite crystals nucleate on the support and grow to form a

---

[*] J. Choi, S. Ghosh, Prof. M. Tsapatsis
Department of Chemical Engineering and Materials Science
University of Minnesota
421 Washington Ave. SE, Minneapolis, MN, 55455 (USA)
Fax: (+1) 612-626-7246
E-mail: tsapatsi@cems.umn.edu
Z. Lai
Division of Chemical and Biomolecular Engineering
Nanyang Technological University
Singapore 637722 (Singapore)

[**] Funding for this work was provided by NSF (CTS-05 22518). All characterizations were performed at the Minnesota Characterization Facility, which receives support from NSF through the National Nanotechnology Infrastructure Network (NNIN).

continuous zeolite layer. At the same time, reactions occurring in the solution lead to deposition of nuclei and crystals on the surface followed by their incorporation into the membrane. MFI films grown in situ may exhibit a preferred orientation that depends on the synthetic protocol and associated interplay of nucleation and growth phenomena.[24] However, because of the insufficient understanding of nucleation and growth processes in hydrothermal systems, the success of in situ methods in yielding uniformly oriented MFI films is limited. In the secondary (or seeded) growth technique, zeolite nucleation is largely decoupled from zeolite growth by predepositing a seed layer of zeolite crystals on the support surface. The seed layer can be deposited with one of the crystallographic directions oriented perpendicular to the support.[20] The seeded surface is then exposed to hydrothermal growth conditions, whereupon the seed crystals grow into a continuous film. At the expense of additional processing steps, this method offers greater flexibility in controlling the orientation of the zeolite crystals and the microstructure of the zeolite membrane, since it decouples nucleation from growth. In principle, the orientation and morphology of the membrane can be manipulated by changing the morphology and orientation of the deposited seed layer and then performing secondary growth under appropriate conditions.

Recently,[20,40] we reported the formation of uniformly *b*-out-of-plane oriented (i.e., with the 5.6×5.4-Å straight pore of MFI perpendicular to the membrane surface) MFI films with by secondary growth of *b*-oriented seed layers. This was achieved by appropriate use of structure-directing agents (SDAs) that act as crystal-shape modifiers to enable the necessary orientation of the seed layer and the appropriate balance between in-plane and out-of-plane growth rates during secondary growth. Herein we present an extension of our approach that allowed the formation of the first continuous MFI films with uniform *a*-out-of-plane orientation, that is, with the 5.1×5.5-Å zigzag channels of MFI perpendicular to the support surface throughout the film thickness.

The procedure follows closely that used for the formation of *b*-oriented films,[20,40] with the main difference being the SDAs used for seed formation and secondary growth. More specifically, the SDA used for seed formation in the procedure leading to *b*-oriented films, that is, tetrapropylammonium hydroxide (TPA), was now used for secondary growth while the SDA that was used for secondary growth in the procedure leading to *b*-oriented films (*N*,*N*-bis(tripropylammoniumhexamethylene)-*N*,*N*-dipropylammonium cation, *trimer*-TPA) was now used for synthesis of the MFI seed crystals. The two processes are illustrated schematically in Figure 1. The procedure for the fabrication of *b*-oriented films has been described in detail before,[20,40] while that for *a*-oriented films is described below.

First, a mesoporous silica layer was prepared on the polished side of an α-alumina porous disk by slip-coating.[40,41] It has been suggested that the silica layer plays several important roles, which include: 1) providing a smooth surface for MFI seed deposition, 2) accommodating a higher density of OH groups than bare α-alumina for bonding the zeolite seed crystals to the substrate, and 3) preventing incorporation of Al from the support in the MFI film during secondary growth. The X-ray diffraction (XRD) patterns of bare porous α-alumina and silica-coated α-alumina are shown in Figure 2a and b, respectively.

To form the *a*-oriented seed layer, MFI crystals were produced in the presence of *trimer*-TPA as SDA.[42] The morphology of these MFI crystals is *b*-elongated leaf-shaped with the order of crystal dimensions $L_c \geq L_b > L_a$, where L_i denotes crystal length along the *i* axis[43,44] (Figure 3a and b). This shape is drastically different from the well-known coffin-shaped MFI crystals with $L_c \geq L_a > L_b$ obtained with TPA as SDA. The difference in crystal morphology is believed to be a direct result of the SDA used, on the basis of the findings of an earlier modeling study.[45] In this study[45] the distinct morphologies obtained with the different SDAs were attributed to the fitting of the SDAs in the straight (along the *b* axis) and sinusoidal channels (along the *a* axis), which correlate with the relative crystal dimensions along the *a* and *b* axes, respectively. More specifically, *trimer*-TPA appears to limit growth along the *a* axis due to the relative difficulty of fitting its long dimension along the *a* axis versus along the *b* axis.[43,44]

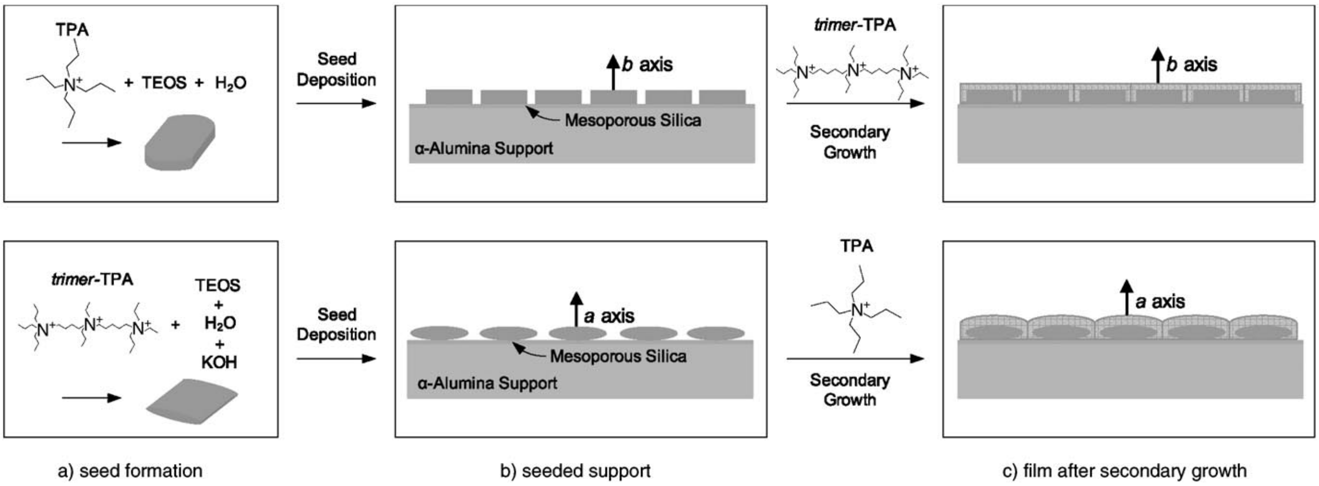

a) seed formation b) seeded support c) film after secondary growth

Figure 1. Schematic representation of the steps used to fabricate MFI films with *b*- and *a*-out-of-plane orientations are shown in the upper and lower panels, respectively.

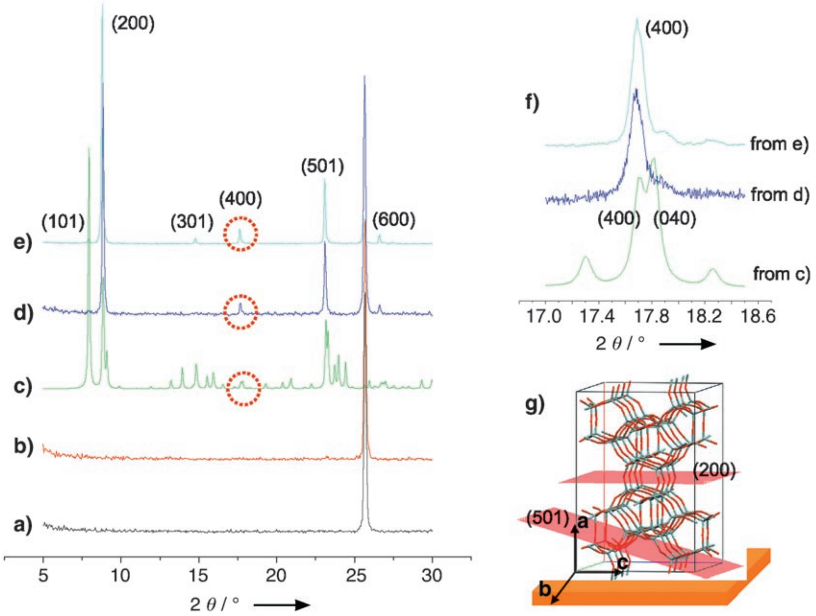

Figure 2. XRD patterns of a) bare porous α-alumina, b) silica-coated α-alumina, c) MFI powder, generated with Mercury Software (Cambridge Crystallographic Data Centre), d) MFI seed monolayer, and e) MFI films after secondary growth. XRD patterns in the 2θ region around the (400) and (040) MFI peaks, indicated by circles in c), d), and e), are shown in f). The MFI unit cell with representative crystallographic planes is shown in g).

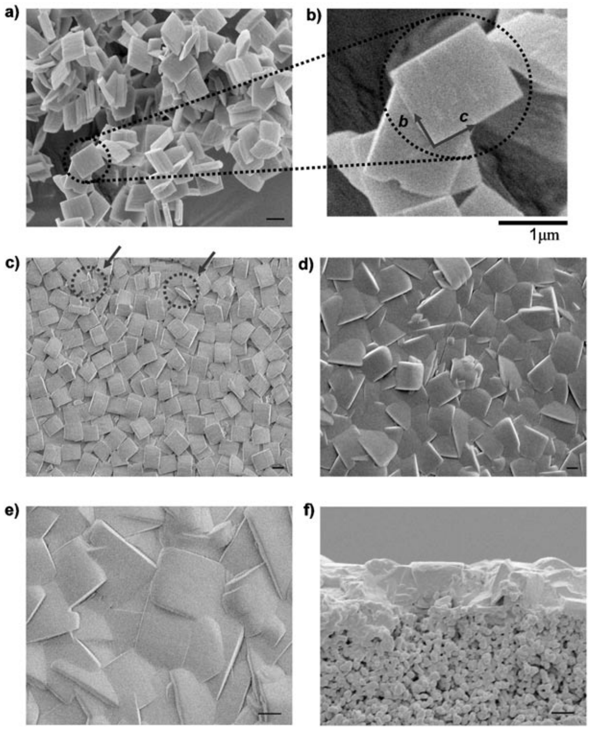

Figure 3. SEM images of a) zeolite MFI crystals obtained with *trimer*-TPA as SDA, b) magnified crystal with indication of *b* and *c* axes, and c) chemically bonded monolayer of MFI seeds after seed deposition with most of the MFI crystals lying flat on the support and few misoriented seeds indicated by arrows. Top-view SEM images of MFI films after secondary growth are shown in d) and e), with lower and higher magnification, respectively, and a cross-sectional view is shown in f). Scale bars are 1 μm.

Following the synthesis of seeds with short dimension along the *a* axis, a monolayer of MFI seeds was formed by bonding zeolite crystals and substrate by the procedure of Yoon and co-workers.[46] The formation of a close-packed nearly monolayer deposit of MFI seeds was evidenced by scanning electron microscopy (SEM, Figure 3c). The majority of MFI crystals rests with their short dimension (*a* axis) perpendicular to the support. A few exceptions of misoriented seed crystals can be found, and representative examples are indicated by arrows in Figure 3c. The *a*-out-of-plane orientation of the monolayer was verified by XRD (Figure 2c, d, and f). Apparently, the anisometric morphology of MFI crystals facilitated deposition with their short dimension (along the *a* axis) perpendicular to the support.

The starting point for the selection of secondary growth conditions was the criterion of comparable in-plane (parallel to the membrane surface) and out-of-plane (perpendicular to the membrane surface) rates.[40] If the out-of-plane growth rate is relatively high, it will lead to films with insufficient grain intergrowth, or large film thickness will be required to obtain intergrown columnar films. On the other hand, if the out-of-plane growth rate is very low then the relatively fast growth of misoriented seeds, twins with *b*-out-of-plane orientation, or randomly oriented nuclei will lead to loss of preferred orientation before a well-intergrown film is achieved. For this reason we selected TPA as SDA and secondary growth conditions of relatively high supersaturation and low temperature to obtain comparable growth rates along the *a* and *c* crystallographic axes of MFI. Screening experiments (not shown) led to selection of secondary growth at 90 °C with a composition of $60\,SiO_2{:}9\,TPAOH{:}9500\,H_2O{:}240\,EtOH$. After hydrothermal secondary growth under the above conditions in the presence of TPA, a continuous MFI film was formed from the *a*-oriented seed layer. Representative SEM top views of a well-intergrown membrane after secondary growth are shown in Figure 3d and e. The thickness of the membrane was estimated to be around 2 μm from cross-sectional views (Figure 3f). The *a*-out-of-plane orientation achieved in seed deposition was preserved during secondary growth, as indicated by the XRD patterns in Figure 2c, e, and f. In these patterns, (*h*00), (301), and (501) MFI reflections (Figure 2g) are present along with the XRD peak from the α-alumina support. The peak of the α-alumina support is still detectable because of the thinness of the zeolite layer, as was the case for thin *b*-oriented film.[20,40] Although some degree of preferred *a*-out-of-plane orientation has been reported before,[39,40,47,48] to our knowledge this is the first time that a uniformly (throughout the membrane thickness) *a*-oriented intergrown MFI film has been fabricated.

In summary, the previously reported procedure for fabrication of *b*-oriented MFI membranes has been extended to acquire *a*-oriented MFI membranes by secondary growth from an *a*-oriented monolayer of MFI seeds. First, MFI crystals were synthesized by using *trimer*-TPA as SDA. The anisometric crystals (thin along the *a* axis) facilitated formation of a close-packed near-monolayer of MFI seeds by chemical bonding on a porous α-alumina substrate coated with mesoporous silica. As a result, an MFI seed layer with *a*-out-of-plane orientation was observed throughout the substrate. During secondary growth in the presence of TPA as SDA, comparable in-plane and out-of-plane growth rates were achieved to obtain well-intergrown *a*-oriented MFI membranes preserving the orientation of the seed layer. Thus, continuous and uniformly *a*-oriented MFI films were fabricated by the methodology of secondary growth and use of SDAs that act as crystal-shape modifiers. It is expected that the approach demonstrated here for siliceous ZSM-5 will also be applicable to other zeolites including cation-substituted ZSM-5. Along with the previously reported *b*-oriented membranes, they provide the first set of uniformly oriented zeolite films. We are currently comparing their permeation properties in an attempt to provide the first set of data for gas and vapor permeation through zeolite membranes of a given structure type with drastically different preferred orientations. Such a data set is expected to be valuable in revealing the relationship between microstructure and membrane performance.

Experimental Section

The synthesis, as well as elemental and NMR analyses, of *trimer*-TPA^{3+}-$3I^-$ were performed as described in reference [43].

Zeolite seeds: The synthesis sol was prepared by dissolving a specific amount of *trimer*-TPA^{3+}-$3I^-$ in deionized water and adding KOH solution (1N, Aldrich). Tetraethyl orthosilicate (TEOS, 98% Aldrich) was added as silica source. The final molar composition of the mixture was $40\,SiO_2$:5(*trimer*-TPA^{3+}-$3I^-$):25 KOH:9500 H_2O:160 EtOH. The mixture was stirred at room temperature overnight and then filtered (qualitative P8, Fisher Scientific) into 45-mL teflon-lined stainless steel autoclaves (Parr). The autoclaves were placed in an oven, preheated to 175 °C. After 24 h, the autoclaves were removed from the oven and quenched in a cold water bath. Solid product was obtained after five repetitions of centrifugation and decantation. The recovered crystals were dried in an oven (ca. 70 °C) and calcined for 10 h at 525 °C with a ramp rate of 1 °C min^{-1}.

Seed deposition: A surfactant-templated silica layer was coated onto a 2-mm-thick α-alumina disk (∅ 22 mm) and calcined for 4 h at 450 °C with a ramp rate of 1 °C min^{-1} (For details on support preparation, see reference [40]). The silica-coated α-alumina was functionalized with (3-chloropropyl)trimethoxysilane (3CP-TMS, 4 mL, 97%, Aldrich) at reflux for 3 h at around 110 °C in dry toluene under argon flow. Calcined and dried MFI seeds (ca. 0.01 g) were dispersed in anhydrous toluene (40 mL) by sonication. The functionalized substrate was then immersed in the toluene/seeds suspension, which was heated to reflux for 3 h at about 110 °C under argon flow. The substrate was sonicated briefly in 30 mL of fresh toluene.

Secondary growth: The molar composition of the synthesis sol was $60\,SiO_2$:9 TPAOH:9500 H_2O:240 EtOH. The synthesis mixture was hydrolyzed for 6 h. The seeded substrate was secured in a 45-mL teflon liner with a slight tilt and the seeded side facing down. The synthesis mixture was then filtered into teflon-lined autoclaves. The autoclaves were placed in an oven preheated to 90 °C and left for 4 days. The films were calcined at 480 °C for 4 h with a ramp rate of 0.5 °C min^{-1}.

Received: August 23, 2005

Keywords: hydrothermal synthesis · monolayers · thin films · zeolites

---

[1] J. Caro, M. Noack, P. Kölsch, R. Schäfer, *Microporous Mesoporous Mater.* **2000**, *38*, 3.
[2] J. Coronas, J. Santamaria, *Catal. Today* **1999**, *51*, 377.
[3] Y. S. Lin, I. Kumakiri, B. N. Nair, H. Alsyouri, *Sep. Purif. Methods* **2002**, *31*, 229.
[4] T. C. Bowen, R. D. Noble, J. L. Falconer, *J. Membr. Sci.* **2004**, *245*, 1.
[5] T. Bein, *Chem. Mater.* **1996**, *8*, 1636.
[6] M. E. Davis, *Nature* **2002**, *417*, 813.
[7] M. Vilaseca, J. Coronas, A. Cirera, A. Cornet, J. R. Morante, J. Santamaria, *Catal. Today* **2003**, *82*, 179.
[8] J. Coronas, J. Santamaria, *Chem. Eng. Sci.* **2004**, *59*, 4879.
[9] J. Coronas, J. Santamaria, *Top. Catal.* **2004**, *29*, 29.
[10] Z. Wang, A. Mitra, H. Wang, L. Huang, Y. Yan, *Adv. Mater.* **2001**, *13*, 1463.
[11] S. Li, C. Demmelmaier, M. Itkis, Z. Liu, R. C. Haddon, Y. Yan, *Chem. Mater.* **2003**, *15*, 2687.
[12] K. Ha, Y.-J. Lee, D.-Y. Jung, J. H. Lee, K. B. Yoon, *Adv. Mater.* **2000**, *12*, 1614.
[13] a) D. Brühwiler, G. Calzaferri, *Microporous Mesoporous Mater.* **2004**, *72*, 1; b) G. Calzaferri, M. Pauchard, H. Maas, S. Huber, A. Khatyr, T. Schaafsma, *J. Mater. Chem.* **2002**, *12*, 1.
[14] J. Caro, F. Marlow, M. Wübbenhorst, *Adv. Mater.* **1994**, *6*, 413.
[15] A. I. Skoulidas, D. S. Sholl, R. Krishna, *Langmuir* **2003**, *19*, 7977.
[16] S. Sommer, T. Melin, J. L. Falconer, R. D. Noble, *J. Membr. Sci.* **2003**, *224*, 51.
[17] C. J. Gump, X. Lin, J. L. Falconer, R. D. Noble, *J. Membr. Sci.* **2000**, *173*, 35.
[18] K. Kusakabe, A. Murata, T. Kuroda, S. Morooka, *J. Chem. Eng. Jpn.* **1997**, *30*, 72.
[19] T. Matsufuji, N. Nishiyama, M. Matsukata, K. Ueyama, *J. Membr. Sci.* **2000**, *178*, 25.
[20] Z. Lai, G. Bonilla, I. Diaz, J. G. Nery, K. Sujaoti, M. A. Amat, E. Kokkoli, O. Terasaki, R. W. Thompson, M. Tsapatsis, D. G. Vlachos, *Science* **2003**, *300*, 456.
[21] J. L. H. Chau, Y. S. S. Wan, A. Gavriilidis, K. L. Yeung, *Chem. Eng. J.* **2002**, *88*, 187.
[22] Z. Wang, Y. Yan, *Microporous Mesoporous Mater.* **2001**, *48*, 229.
[23] Z. Wang, Y. Yan, *Chem. Mater.* **2001**, *13*, 1101.
[24] S. Li, Z. Li, K. N. Bozhilov, Z. Chen, Y. Yan, *J. Am. Chem. Soc.* **2004**, *126*, 10732.
[25] A. Gouzinis, M. Tsapatsis, *Chem. Mater.* **1998**, *10*, 2497.
[26] M. C. Lovallo, M. Tsapatsis, *AIChE J.* **1996**, *42*, 3020.
[27] G. Xomeritakis, A. Gouzinis, S. Nair, T. Okubo, M. He, R. M. Overney, M. Tsapatsis, *Chem. Eng. Sci.* **1999**, *54*, 3521.
[28] J. H. Koegler, H. van Bekkum, J. C. Jansen, *Zeolites* **1997**, *19*, 262.
[29] F.-Z. Zhang, M. Fuji, M. Takahashi, *Chem. Mater.* **2005**, *17*, 1167.
[30] T. Seike, M. Matsuda, M. Miyake, *J. Am. Ceram. Soc.* **2004**, *87*, 1585.
[31] W. C. Wong, L. T. Y. Au, C. T. Ariso, K. L. Yeung, *J. Membr. Sci.* **2001**, *191*, 143.
[32] L. T. Y. Au, K. L. Yeung, *J. Membr. Sci.* **2001**, *194*, 33.
[33] L. H. Chau, W. C. Wong, K. L. Yeung, *Fifth International Conference on Inorganic Membranes*, Nagoya, Japan, **1998**, pp. 432.
[34] J. Sun, G. Zhu, X. Yin, Y. Chen, Y. Cui, S. Qiu, *Chem. Commun.* **2005**, 1070.
[35] S. Mintova, V. Valtchev, V. Engström, B. J. Schoeman, J. Sterte, *Microporous Mater.* **1997**, *11*, 149.
[36] S. Mintova, J. Hedlund, V. Valtchev, B. J. Schoeman, J. Sterte, *J. Mater. Chem.* **1998**, *8*, 2217.
[37] S. Mintova, T. Bein, *Adv. Mater.* **2001**, *13*, 1880.

[38] H. W. Deckman, E. W. Corcoran, Jr., J. A. Mchenry, W. F. Lai, L. R. Czarnetzki, W. E. Wales (Exxon Research and Engineering Company), WO 96/01686, **1996**, [*Chem. Abstr.* **1996**, *124*, 180384p].

[39] J. P. Verduijn, A.-J. Bons, M. H. C. Anthonis, L. R. Czarnetzki (Exxon Chemical Patents Inc.), WO 96/01683, **1996**, [*Chem. Abstr.* **1996**, *124*, 236420s].

[40] Z. Lai, M. Tsapatsis, J. P. Nicolich, *Adv. Funct. Mater.* **2004**, *14*, 716.

[41] Y. Lu, R. Ganguli, C. A. Drewien, M. T. Anderson, C. J. Brinker, W. Gong, Y. Guo, H. Soyez, B. Dunn, M. H. Huang, J. I. Zink, *Nature* **1997**, *389*, 364.

[42] L. W. Beck, M. E. Davis, *Microporous Mesoporous Mater.* **1998**, *22*, 107.

[43] G. Bonilla, I. Díaz, M. Tsapatsis, H.-K. Jeong, Y. Lee, D. G. Vlachos, *Chem. Mater.* **2004**, *16*, 5697.

[44] I. Díaz, E. Kokkoli, O. Terasaki, M. Tsapatsis, *Chem. Mater.* **2004**, *16*, 5226.

[45] E. de Vos Burchart, J. C. Jansen, B. van de Graaf, H. van Bekkum, *Zeolites* **1993**, *13*, 216.

[46] a) K. Ha, Y.-J. Lee, H. J. Lee, K. B. Yoon, *Adv. Mater.* **2000**, *12*, 1114; b) S. Y. Choi, Y. J. Lee, Y. S. Park, K. Ha, K. B. Yoon, *J. Am. Chem. Soc.* **2000**, *122*, 5201; c) A. Kulak, Y. J. Lee, Y. S. Park, K. B. Yoon, *Angew. Chem.* **2000**, *112*, 980; *Angew. Chem. Int. Ed.* **2000**, *39*, 950; d) G. S. Lee, Y. J. Lee, K. B. Yoon, *J. Am. Chem. Soc.* **2001**, *123*, 9769; e) J. S. Park, G. S. Lee, Y. J. Lee, Y. S. Park, K. B. Yoon, *J. Am. Chem. Soc.* **2002**, *124*, 13366; f) J. S. Park, Y. J. Lee, K. B. Yoon, *J. Am. Chem. Soc.* **2004**, *126*, 1934.

[47] J. Hedlund, S. Mintova, J. Sterte, *Microporous Mesoporous Mater.* **1999**, *28*, 185.

[48] J. S. Lee, Y.-J. Lee, E. L. Tae, Y. S. Park, K. B. Yoon, *Science* **2003**, *301*, 818.